

# A simple, narrow, and robust atomic frequency reference at 993 nm exploiting the rubidium (Rb) $5S_{1/2}$ to $6S_{1/2}$ transition using one-color two-photon excitation

THOMAS NIEDDU,<sup>1</sup> TRIDIB RAY,<sup>1</sup> KRISHNAPRIYA S. RAJASREE,<sup>1</sup>  
RITAYAN ROY,<sup>2,\*</sup> AND SÍLE NIC CHORMAIC<sup>1, 3, 4</sup>

<sup>1</sup>*Light-Matter Interactions Unit, Okinawa Institute of Science and Technology Graduate University, Onna, Okinawa 904-0495, Japan*

<sup>2</sup>*Quantum Systems & Devices Group, School of Mathematical and Physical Sciences, Pevensey II, University of Sussex, Falmer, Brighton, BN1 9QH, UK*

<sup>3</sup>*Université Grenoble Alpes, CNRS, Grenoble INP, Institut Néel, 38000 Grenoble, France*

<sup>4</sup>*School of Chemistry and Physics, University of KwaZulu-Natal, Durban 4001, South Africa*

\**ritayan.roy@u.nus.edu*

**Abstract:** We experimentally demonstrate a one-color two-photon transition from the  $5S_{1/2}$  ground state to the  $6S_{1/2}$  excited state in rubidium (Rb) vapor using a continuous wave laser at 993 nm. The Rb vapor contains both isotopes ( $^{85}\text{Rb}$  and  $^{87}\text{Rb}$ ) in their natural abundances. The electric dipole allowed transitions are characterized by varying the power and polarization of the excitation laser. Since the optical setup is relatively simple, and the energies of the allowed levels are impervious to stray magnetic fields, this is an attractive choice for a frequency reference at 993 nm, with possible applications in precision measurements and quantum information processing.

© 2018 Optical Society of America

## References and links

1. K. Shimoda, *High-Resolution Laser Spectroscopy*, Topics in Applied Physics (Springer Berlin Heidelberg, 2014).
2. L. S. Vasilenko, V. P. Chebotaev, and A. V. Shishaev, "Line shape of two-photon absorption in a standing-wave field in a gas," *JETP Letters* **12**, 113 – 115 (1970).
3. B. Cagnac, G. Grynberg, and F. Biraben, "Spectroscopie d'absorption multiphotonique sans effet Doppler," *Journal de Physique* **34**, 845–858 (1973).
4. N. Bloembergen, M. D. Levenson, and M. M. Salour, "Zeeman effect in the two-photon  $3S - 5S$  transition in sodium vapor," *Phys. Rev. Lett.* **32**, 867–869 (1974).
5. T. W. Hänsch, "Nobel lecture: Passion for precision," *Rev. Mod. Phys.* **78**, 1297–1309 (2006).
6. S. Gulde, H. Häffner, M. Riebe, G. Lancaster, C. Becher, J. Eschner, F. Schmidt-Kaler, I. L. Chuang, and R. Blatt, "Quantum information processing with trapped  $\text{Ca}^+$  ions," *Philosophical Transactions of the Royal Society of London A: Mathematical, Physical and Engineering Sciences* **361**, 1363–1374 (2003).
7. I. D. Abella, "Optical double-photon absorption in cesium vapor," *Phys. Rev. Lett.* **9**, 453–455 (1962).
8. F. Biraben, B. Cagnac, and G. Grynberg, "Observation of the  $3S - 5S$  two-photon transition in sodium vapor without Doppler broadening, using a CW dye laser," *Physics Letters A* **49**, 71 – 72 (1974).
9. D. Roberts and E. Fortson, "Rubidium isotope shifts and hyperfine structure by two-photon spectroscopy with a multi-mode laser," *Optics Communications* **14**, 332 – 335 (1975).
10. E. Campani, G. Degan, G. Gorini, and E. Polacco, "Measurement of the  $8S$  hyperfine splitting in cesium," *Optics Communications* **24**, 203 – 206 (1978).
11. Y.-W. Liu and P. E. G. Baird, "Two-photon spectroscopy in potassium," *Measurement Science and Technology* **12**, 740 (2001).
12. B. A. Bushaw, W. Nörtershäuser, G. Ewald, A. Dax, and G. W. F. Drake, "Hyperfine splitting, isotope shift, and level energy of the  $3S$  states of  $^{6,7}\text{Li}$ ," *Phys. Rev. Lett.* **91**, 043004 (2003).
13. M.-S. Ko and Y.-W. Liu, "Observation of rubidium  $5S_{1/2} \rightarrow 7S_{1/2}$  two-photon transitions with a diode laser," *Opt. Lett.* **29**, 1799–1801 (2004).
14. Y.-C. Lee, Y.-H. Chang, Y.-Y. Chen, C.-C. Tsai, and H.-C. Chui, "Polarization and pressure effects in caesium  $6S-8S$  two-photon spectroscopy," *Journal of Physics B: Atomic, Molecular and Optical Physics* **43**, 235003 (2010).
15. T. W. Hänsch, S. A. Lee, R. Wallenstein, and C. Wieman, "Doppler-free two-photon spectroscopy of hydrogen  $1s - 2s$ ," *Phys. Rev. Lett.* **34**, 307–309 (1975).

16. A. Matveev, C. G. Parthey, K. Predehl, J. Alnis, A. Beyer, R. Holzwarth, T. Udem, T. Wilken, N. Kolachevsky, M. Abgrall, D. Rovera, C. Salomon, P. Laurent, G. Grosche, O. Terra, T. Legero, H. Schnatz, S. Weyers, B. Altschul, and T. W. Hänsch, “Precision measurement of the hydrogen  $1S - 2S$  frequency via a 920-km fiber link,” *Phys. Rev. Lett.* **110**, 230801 (2013).
17. R. Roy, P. C. Condyllis, Y. J. Johnathan, and B. Hessmo, “Atomic frequency reference at 1033 nm for ytterbium (Yb)-doped fiber lasers and applications exploiting a rubidium (Rb)  $5S_{1/2}$  to  $4D_{5/2}$  one-colour two-photon transition,” *Opt. Express* **25**, 7960–7969 (2017).
18. T. Chanelière, D. N. Matsukevich, S. D. Jenkins, T. A. B. Kennedy, M. S. Chapman, and A. Kuzmich, “Quantum telecommunication based on atomic cascade transitions,” *Phys. Rev. Lett.* **96**, 093604 (2006).
19. K. D. Bonin and T. J. McIlrath, “Two-photon electric-dipole selection rules,” *J. Opt. Soc. Am. B* **1**, 52–55 (1984).
20. A. Pérez Galván, Y. Zhao, and L. A. Orozco, “Measurement of the hyperfine splitting of the  $6S_{1/2}$  level in rubidium,” *Phys. Rev. A* **78**, 012502 (2008).
21. Grynberg, G., Biraben, F., Giacobino, E., and Cagnac, B., “Doppler-free two-photon spectroscopy of neon. ii. line intensities,” *J. Phys. France* **38**, 629–640 (1977).
22. G. Grynberg and B. Cagnac, “Doppler-free multiphotonic spectroscopy,” *Reports on Progress in Physics* **40**, 791 (1977).
23. E. Gomez, S. Aubin, L. A. Orozco, and G. D. Sprouse, “Lifetime and hyperfine splitting measurements on the  $7S$  and  $6P$  levels in rubidium,” *J. Opt. Soc. Am. B* **21**, 2058–2067 (2004).
24. E. Gomez, F. Baumer, A. D. Lange, G. D. Sprouse, and L. A. Orozco, “Lifetime measurement of the  $6S$  level of rubidium,” *Phys. Rev. A* **72**, 012502 (2005).
25. C. S. Wood, S. C. Bennett, J. L. Roberts, D. Cho, and C. E. Wieman, “Precision measurement of parity nonconservation in cesium,” *Canadian Journal of Physics* **77**, 7–75 (1999).
26. J. Guéna, D. Chauvat, P. Jacquier, E. Jahier, M. Lintz, S. Sanguinetti, A. Wasan, M. A. Bouchiat, A. V. Papoyan, and D. Sarkisyan, “New manifestation of atomic parity violation in cesium: A chiral optical gain induced by linearly polarized  $6S-7S$  excitation,” *Phys. Rev. Lett.* **90**, 143001 (2003).
27. R. T. Willis, F. E. Becerra, L. A. Orozco, and S. L. Rolston, “Correlated photon pairs generated from a warm atomic ensemble,” *Phys. Rev. A* **82**, 053842 (2010).
28. T. Nieddu, V. Gokhroo, and S. Nic Chormaic, “Optical nanofibres and neutral atoms,” *Journal of Optics* **18**, 053001 (2016).
29. H. You, S. M. Hendrickson, and J. D. Franson, “Analysis of enhanced two-photon absorption in tapered optical fibers,” *Phys. Rev. A* **78**, 053803 (2008).

---

## 1. Introduction

Two-photon processes in atomic systems have several distinct advantages over single-photon processes. For example, two-photon processes can give direct access to optical excitations that would be electric-dipole forbidden for a single-photon process [1]. Furthermore, when the two photons are derived from two laser beams in a counter-propagating configuration, a judicious choice of the polarizations can yield background-less, Doppler-free spectra [2, 3]. In addition, two-photon transition frequencies for  $S$  to  $S$  transitions are insensitive to magnetic fields below the Paschen-Back domain [4], while two-photon transitions to metastable states have extremely narrow linewidths compared to those for single-photon processes [5, 6]. These unique features make two-photon spectroscopy a powerful tool for precision measurements. Following the first observation of a two-photon transition in an atomic system containing cesium [7], numerous different atomic transitions have been investigated [8–14]. The technique has been extensively used for metrology and the accurate determination of fundamental constants [15, 16], as a frequency reference [17], and in quantum telecommunications [18].

In this paper, we report on the observation and spectroscopic study of the  $5S_{1/2}$  to  $6S_{1/2}$  two-photon transition in a hot Rb-atom vapor using a single-frequency laser beam. To our knowledge, this is the first observation of this particular Rb transition using a one-color two-photon excitation. We explore the dependency of the spectroscopy signal on (i) the intensity and (ii) the polarization of the pump beam. Observation of a quadratic dependency on the intensity of the pump laser is a signature of the two-photon transition. We also show that the pump laser frequency can be stabilized to the observed spectroscopic peaks, thereby illustrating that the transition can be used as a frequency reference. Finally, we discuss some possible applications for precision measurements and quantum telecommunications.

## 2. Experimental Details

The energy level diagram for the Rb transition of interest is shown in Fig. 1. Atoms are excited from the  $5S_{1/2}$  ground state via a virtual state to the  $6S_{1/2}$  state using a two-photon process at 993 nm. The atoms can decay back to the ground state via two possible channels characterized by an intermediate state, which can be either (i) the  $5P_{1/2}$  level on emission of a pair of photons with wavelengths of 1324 nm and 795 nm (i.e. the D1 transition), or (ii) the  $5P_{3/2}$  level on emission of a pair of photons with wavelengths of 1367 nm and 780 nm (i.e. the D2 transition). The photons at 1324 nm and 1367 nm fall beyond the range of the detectors available for this experiment, hence, for the work reported hereafter, we only detect the 780 nm and 795 nm light.

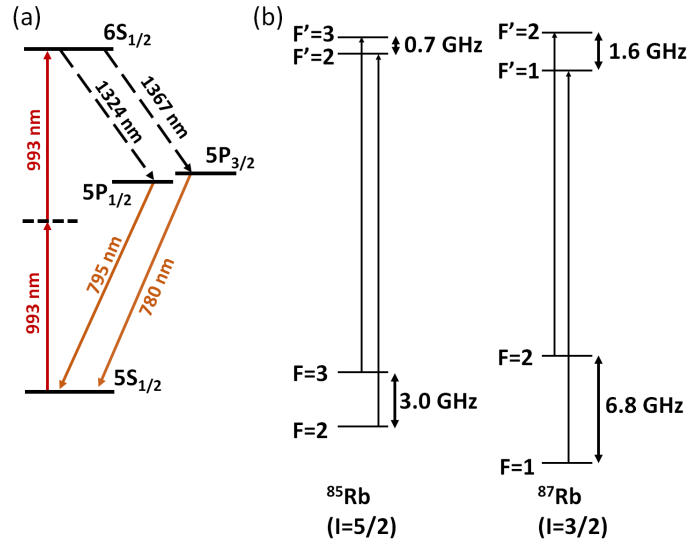


Fig. 1. (a) Energy level diagram for Rb. A beam at 993 nm excites atoms from  $5S_{1/2}$  to  $6S_{1/2}$  via single-color two-photon excitation. The intermediate virtual state is represented as a dashed line. The atoms decay back to  $5S_{1/2}$  via  $5P_{1/2}$  or  $5P_{3/2}$ , with photons emitted at 795 nm and 780 nm (orange arrows); (b) Hyperfine level diagrams for the two Rb isotopes. Two-photon transitions allowed by the selection rule,  $\Delta F = 0$ ,  $\Delta m_F = 0$ , are shown, along with the frequencies of the hyperfine splittings.

The experimental setup is illustrated in Fig. 2. The experiment is carried out in a glass cell filled with Rb in its natural isotopic abundances, maintained at a temperature of 130 °C. The 993 nm beam used to drive the two-photon transition is provided by a continuous wave (CW) Ti:Sapphire laser (Coherent MBR 110), locked to a scanning reference cavity yielding a spectral linewidth of 100 kHz. The laser frequency can be scanned by changing the length of the reference cavity. The combination of a half-wave plate (HWP) and a polarizing beam-splitter (PBS) at the output of the laser allows us to control the powers in the reflected (R) and transmitted (T) beams from the PBS. Most of the optical power, typically >90%, is in T and passes through the vapor cell for the two-photon spectroscopy studies. The remaining light, in R, is fiber-coupled and further split so that 99% goes to a Fabry-Pérot cavity (Toptica FPI-100) and 1% to a wavemeter (HighFinesse WS-6). The wavemeter has two purposes; it allows us to tune the laser to the desired wavelength and to monitor the frequency scanning. The Fabry-Pérot cavity has a free-spectral range of 1 GHz and is used to monitor the linearity of the frequency scan.

An optical isolator is placed before the vapor cell to avoid reflections back into the laser. A plano-convex lens (L1), with focal length  $f_1 = 150$  mm, is placed after the optical isolator to

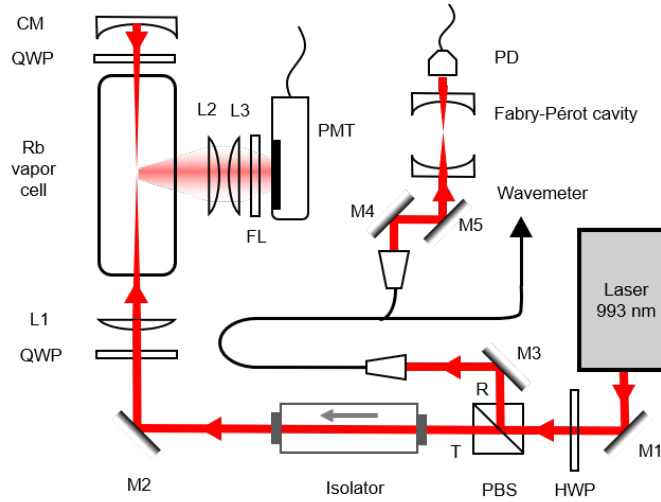


Fig. 2. Schematic of the experimental setup. Light from a tunable 993 nm laser is used for two-photon excitation in a Rb vapor cell using a retro-reflected configuration. The resulting atomic fluorescence is detected by a PMT. The polarizations of the forward and retro-reflected beams are controlled using QWPs. A small amount (i.e.  $<10\%$ ) of the 993 nm beam is coupled to a Fabry-Pérot cavity and a wavemeter to monitor the laser frequency. M1-M5: Mirrors, L1-L3 Plano-convex lens, HWP: Half-wave plate, QWP: Quarter-wave plate, PBS: Polarizing beam splitter, CM: Concave mirror, PMT: Photomultiplier tube, FL: Short-pass optical filter, PD: Photodiode.

focus the beam in the cell. The  $1/e^2$  beam diameter is  $128 \mu\text{m}$ . A concave mirror (CM), with focal length  $f_{CM} = 75 \text{ mm}$ , and placed  $2f_{CM} = 150 \text{ mm}$  away from the focal plane of L1 ensures retro-reflection of the beam back to the focal point. Quarter-wave plates (QWP) can be inserted in the beam path before L1 and CM to generate a circularly polarized beam. We detect both the 795 nm and 780 nm decay photons using a photomultiplier tube (PMT) (Hamamatsu R636-10). A short-pass filter with a cut-off wavelength of 800 nm is placed in front of the PMT to prevent any scattered light from the 993 nm pump from being detected. We use a pair of lenses, L2 and L3, with focal lengths of  $f_2 = f_3 = 50 \text{ mm}$ , in front of the PMT in a telescope configuration for efficient collection of the light. The quantum efficiencies of the PMT at 780 nm and 795 nm are 9% and 8%, respectively. The obtained current is amplified by a pre-amplifier with a gain of  $10^5$  and dropped across a  $50 \Omega$  resistor on an oscilloscope.

### 3. Results

Electric dipole allowed two-photon transitions from  $S$  to  $S$  levels obey the selection rules  $\Delta F = 0$  and  $\Delta m_F = 0$  [19]. This results in only two allowed transitions for each Rb isotope, i.e.  $^{87}\text{Rb } F = 2 - F' = 2$ ,  $^{85}\text{Rb } F = 3 - F' = 3$ ,  $^{85}\text{Rb } F = 2 - F' = 2$ , and  $^{87}\text{Rb } F = 1 - F' = 1$  (see Fig. 1(b)). A typical spectrum obtained is shown in Fig. 3(a). Here, excitation to the  $6S_{1/2}$  level is obtained by scanning the frequency of the 993 nm laser and using the same linear polarization for the forward and retro-reflected beams that generate the two-photon process. Note that the simple setup presented here does not measure the absolute frequency of the transition. The hyperfine splitting of the  $6S_{1/2}$  level is obtained from Ref. [20] using a resonant intermediate level. The relative frequency difference is obtained by setting the frequency of the first peak, i.e. the  $^{87}\text{Rb } 5S_{1/2}, F = 2 - 6S_{1/2}, F' = 2$  transition, to zero, see Fig. 3(a). A linear frequency scaling obtained by using fringe interpolation of the Fabry-Pérot peaks, which are 1 GHz apart, yields a similar

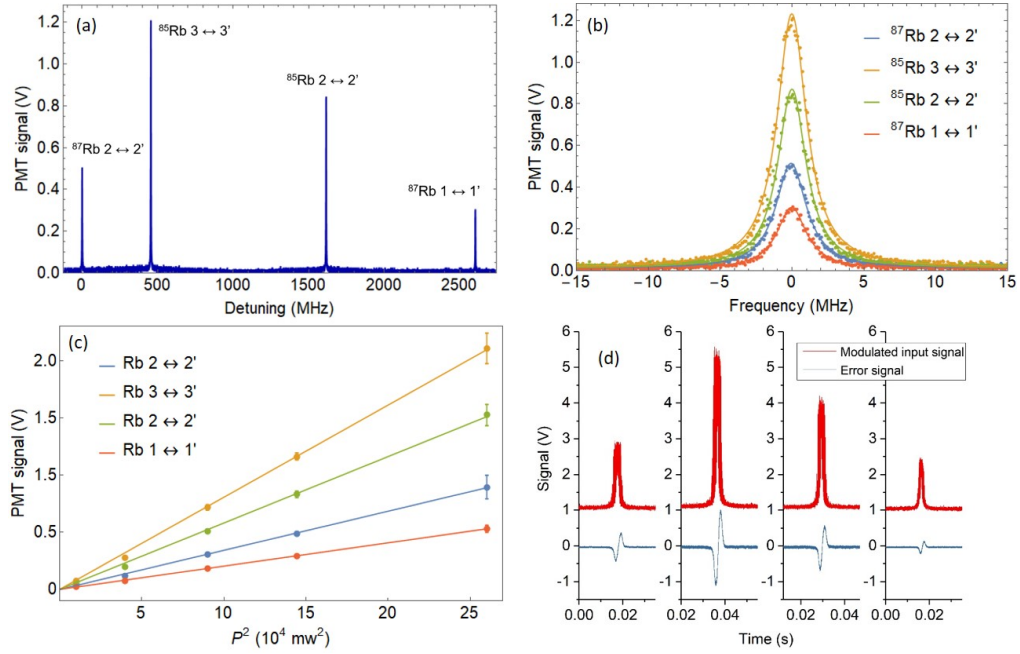


Fig. 3. (a) Typical spectroscopic signal obtained by scanning the frequency of the 993 nm pump beam and recording the signal on the PMT. Each peak indicates a hyperfine transition as labeled. (b) Comparison of the individual peak intensities and linewidths from (a). (c) Linear dependence of the peak height as a function of the total pump power ( $P$ ) squared. (d) Modulated signals and the generated error signals for each peak to which the laser can be locked. For clarity, a 1 V offset is added to the modulated signal.

result. Due to the two-photon process, the relative frequency differences of the peaks are half the actual energy differences of the atomic levels.

### 3.1. Power variation

The relative height and width of each peak in Fig. 3(a) is shown in Fig. 3(b). For a particular Rb isotope, the intensities of the transitions from the ground hyperfine levels are proportional to the statistical weights of the atomic population in those hyperfine levels [21]. However, since the difference in energy between the hyperfine levels is negligible compared to the transition energy, the weight factor is equivalent to the degeneracy ( $2F + 1$ ) of the hyperfine levels. These values are 5 : 3 and 7 : 5 for  $^{87}\text{Rb}$  and  $^{85}\text{Rb}$ , respectively. The variation of peak height as a function of the square of the laser power is shown in Fig. 3(c). The peak heights show a quadratic dependence on the total beam power,  $P$  (i.e. the sum of the powers in the forward and retro-reflected beams); this is a signature of the two-photon process [22]. The ratios of the slopes of the fitted straight lines are 1.667 for  $^{87}\text{Rb}$  and 1.387 for  $^{85}\text{Rb}$ , i.e., close to the expected ratios of 5 : 3 and 7 : 5, respectively. The width of the peaks does not change as a function of power, at least within the standard deviation of the measurements. We measure a Lorentzian full-width-at-half-maximum (FWHM) of  $2.60 \pm 0.07$  MHz,  $2.44 \pm 0.09$  MHz,  $2.49 \pm 0.04$  MHz and  $2.43 \pm 0.04$  MHz for  $^{87}\text{Rb } F = 2 - F' = 2$ ,  $^{87}\text{Rb } F = 1 - F' = 1$ ,  $^{85}\text{Rb } F = 3 - F' = 3$  and  $^{85}\text{Rb } F = 2 - F' = 2$  peaks, respectively.

### 3.2. Laser frequency stabilization to spectroscopic peaks

To establish the viability of the transition as a frequency reference, we demonstrate frequency locking of the pump laser to the spectroscopic peaks. This is implemented by integrating a TEM LaseLock<sup>®</sup> module with the Ti:Sapphire laser. First, the reference cavity is bypassed and the laser frequency is scanned by directly scanning its cavity. A 10 kHz modulation is applied to one of the piezo-driven mirrors to generate frequency sidebands. The modulated spectroscopic signal is fed into a lock-in amplifier and an error signal is generated. An example of a modulated signal and a derived error signal are shown in Fig. 3(d). The laser cavity and, hence, the frequency can be stabilized to each of these error signals.

### 3.3. Polarization variation

We next explore the effect of changing the polarization of the counter-propagating beams on the spectroscopic signal. As shown in Fig. 2, a quarter-wave plate at either end of the vapor cell can be used to generate identical, or orthogonal, circularly polarized forward and retro-reflected beams. Let us denote linear and circular polarizations as  $\pi$  and  $\sigma$ , respectively, and their orthogonal polarizations as  $\pi'$  and  $\sigma'$ , respectively. As mentioned, the two-photon transition selection rules between the  $S$  levels are  $\Delta F = 0$  and  $\Delta m_F = 0$ , hence the total angular momentum of two photons absorbed by an atom during the excitation process must be zero.

First we study the case of linear polarizations. By blocking the retro-reflected beam, a  $\pi$  configuration is created, see Fig. 4(a). We observe a Doppler-broadened signal since both photons are derived from the forward beam. Next, by introducing a retro-reflected beam, a  $\pi - \pi$  configuration is created, see Fig. 4(b). Here, we obtain a narrow Doppler-free spectrum on top of a small Doppler-broadened baseline. The Doppler-free spectrum arises when the two photons are absorbed from counter-propagating beams, whereas the Doppler-broadened signal results from the two photons being absorbed from the same (forward or retro-reflected) beam. Next, the addition of a QWP after the vapor cell, aligned at  $45^\circ$  with respect to the forward beam's polarization axis, creates a linearly polarized, retro-reflected beam, orthogonal to the forward beam, resulting in a  $\pi - \pi'$  configuration, see Fig. 4(c). In this case, the two photons can only be absorbed from either the forward or the retro-reflected beam, i.e., they cannot be absorbed simultaneously from both beams. This results in a signal on the PMT that is the sum of two Doppler-broadened spectra, one from each beam, yielding double the amplitude of the  $\pi$  configuration.

We next move to the case where the beams have circular polarizations. By inserting a QWP at  $45^\circ$  before the vapor cell and blocking the retro-reflected beam, a  $\sigma$  configuration (see Fig. 4(d)) is created. In this case, the transition is forbidden (the sum of the angular momenta of two photons in the forward beam is non-zero), hence there is no signal recorded on the PMT. The  $\sigma - \sigma$  configuration (see Fig. 4(e)) is created by allowing the retro-reflected beam to propagate inside the vapor cell. This transition is also forbidden as, once more, the sum of the angular momenta of the two photons from the counter-propagating beams ( $2\hbar$ ) is non-zero; as a result there is no signal. Finally, inserting a QWP before the retro-reflecting mirror forms a  $\sigma - \sigma'$  configuration. The orientation of the waveplate's axis is irrelevant. The two photons that drive the transition can only be absorbed from the counter-propagating beams. As a result, a background-less, Doppler-free spectrum is obtained (Fig. 4(f)). The peak heights are half those obtained for the  $\pi - \pi$  configuration as the probability to absorb two-photons with opposite spin angular momentum is lesser in this case. It should be noted that the other orthogonal circular polarization configuration yields a similar result and is not presented here.

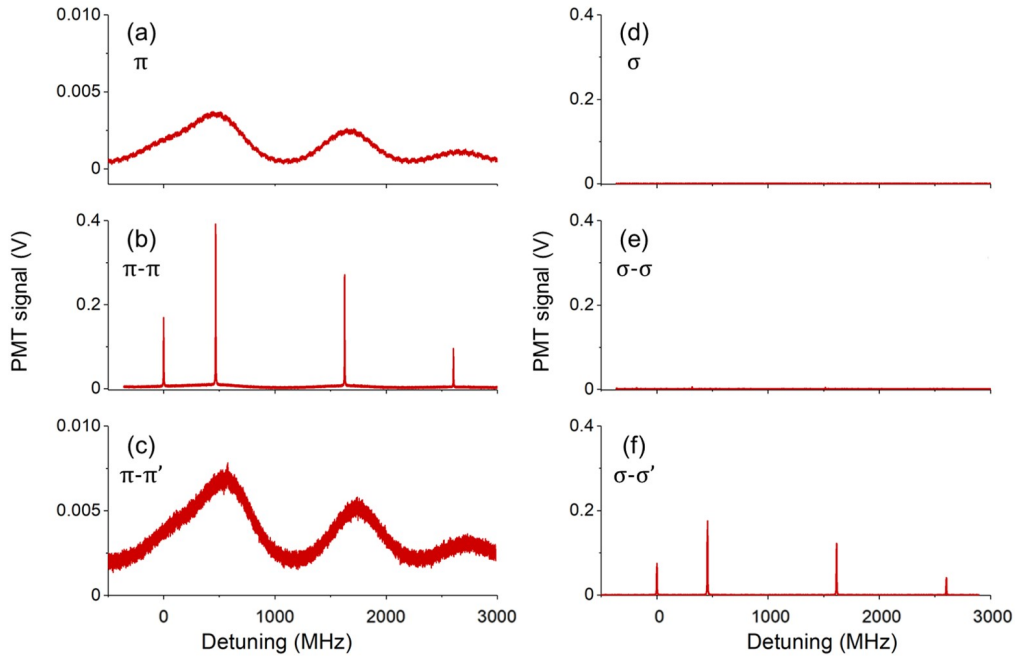


Fig. 4. Effect of beam polarization on the two-photon excitation as recorded by the PMT. As in Fig. 3(a), the relative frequency is obtained by setting the frequency of the  $5S_{1/2}, F = 2 - 6S_{1/2}, F' = 2$  peak to zero. The power of the 993 nm beam is fixed at 250 mW and its frequency is scanned. The polarization of the beam is changed using QWPs. (a) Doppler-broadened spectrum with a single, linearly polarized beam. (b) Linearly polarized counter-propagating beams reveal the Doppler-free peaks and a small Doppler-broadened base. (c) Counter-propagating beams with orthogonal linear polarizations yield a Doppler-broadened spectrum of twice the amplitude of that in (a). (d) A single, circularly polarized beam does not yield a signal. This configuration is forbidden, according to the selection rules. (e) Counter-propagating beams with identical circular polarizations do not yield a signal for the same reason as in (d). (f) Counter-propagating beams with orthogonal circular polarizations yield a background-less Doppler-free spectrum. Here, the total angular momentum for the transition is zero.

#### 4. Discussion

*Ab-initio* calculations of the electronic wavefunction close to the nucleus rely on an accurate measurement of the hyperfine splitting of the atomic energy level [23]. To date, the  $6S_{1/2}$  level in Rb has been accessed via a two-color, two-photon excitation scheme at 795 nm and 1324 nm for measuring its lifetime [20] and hyperfine splitting [24]. Accessing the  $6S_{1/2}$  level via the one-color, two-photon method presented here should enhance the accuracy and precision of such measurements since only a single laser is necessary for the excitation. Additionally, the two-photon transition could be used for the measurement of parity nonconservation [25, 26] in alkali atoms.

The excitation scheme presented herein enables the conversion of two near-infrared photons at 993 nm into a telecommunication O-band photon, at either 1324 nm or 1367 nm, and another near-infrared photon, at 795 nm or 780 nm, respectively. Chaneilière *et al.* [18] proposed a method for building quantum repeaters using cascaded atomic transitions, whereas Willis *et al.* [27] generated time-correlated photon-pairs between a near-infrared photon and an O-band photon

using a four-wave mixing (4WM) process in a Rb vapor. The 4WM scheme made use of the  $6S_{1/2}$  level, accessed via a two-color, two-photon excitation. Our scheme is compatible with these results, as driving the  $5S_{1/2}$  to  $6S_{1/2}$  two-photon transition would permit us to exploit both O-band photons as signal photons, and the corresponding NIR photons as idlers mapped onto an atomic quantum memory. In particular, the 993 nm photons could be coupled to atoms interacting with the evanescent field at the waist of an optical nanofiber embedded in a cold atomic ensemble [28] to make the process more efficient [29].

The first order Zeeman shifts experienced by the same hyperfine states of the  $5S_{1/2}$  and  $6S_{1/2}$  levels are identical since they have the same hyperfine Landé  $g$ -factors. This feature renders the frequency of the  $5S_{1/2}$  to  $6S_{1/2}$  transition insensitive to stray magnetic fields. The transition frequency is also less sensitive to electric fields compared to transitions to nonzero angular momentum states (where  $l > 0$ ). These features makes the transition an attractive choice for a frequency reference.

## 5. Conclusion

We have demonstrated the  $5S_{1/2}$  to  $6S_{1/2}$  one-color, two-photon transition in a hot Rb vapor. The effects of excitation laser power and beam polarization on the observed spectroscopy signals were investigated. We also propose that the transition can be used as a reference at 993 nm by demonstrating frequency stabilization of the excitation laser to the spectroscopic peaks. The simple optical setup is easy to miniaturize and can be readily integrated into more complex experiments. The transition frequency is insensitive to stray magnetic fields and is, therefore, suitable for precision measurements and experimental setups where magnetic fields cannot be completely eliminated, e.g. in a magneto-optical trap or a magnetically trapped Bose-Einstein condensate. Future investigation of the enhanced nonlinear process by embedding an optical nanofiber in such a system will open up new possibilities for the generation of a fiber-integrated photon-pair source for quantum key distribution.

## Funding

This work is supported by the Okinawa Institute of Science and Technology Graduate University.

## Acknowledgments

R. Roy would like to thank B.Hessmo for discussion.